Cortical Microtubule Arrays Lose Uniform Alignment Between Cells and are Oryzalin Resistant in the Arabidopsis Mutant, *radially swollen 6*

Alex Bannigan [1, 4, *], **Allison M. D. Wiedemeier** [2], **Richard E. Williamson** [3], **Robyn L. Overall** [4] **and Tobias I. Baskin** [1]

[1] *Biology Department, University of Massachusetts, Amherst, MA, USA*
[2] *Division of Biological Sciences, University of Missouri, Columbia, MO, USA*
[3] *Plant Cell Biology Group, Australian National University, Canberra, ACT, Australia*
[4] *School of Biological Sciences, University of Sydney, NSW, Australia*

The coordinated expansion of cells is essential to the formation of correctly shaped plant tissues and organs. Members of the *radially swollen* (*rsw*) class of temperature-sensitive arabidopsis mutants were isolated in a screen for reduced anisotropic expansion, by selecting plants with radially swollen root tips. Here we describe *rsw6*, in which cortical microtubules in the root epidermis are well organized in parallel arrays within cells, but neighboring cells frequently contain arrays differing in their mean orientation by up to 90°. Microtubules in *rsw6* are more resistant to oryzalin-induced depolymerization than wild-type microtubules, and their reorientation is accompanied by swelling of the epidermal cells. The reorientation phenotype is blocked by taxol and by the depolymerization of actin filaments. We propose that *rsw6* microtubule organization is functional on a local level, but defective on a global scale. The *rsw6* mutant provides a unique tool with which to study the coordination of microtubule organization at a multicellular level.

Introduction

In plants, the formation and maintenance of consistently shaped organs and tissues depends on the direction and extent of expansion of individual cells, and also on the coordination of that expansion between cells. For morphogenesis, each cell's growth must fit in with the overall body plan of the plant.

The control of plant cell expansion is, at least in part, determined by the organization and dynamics of the cortical microtubule array, which lies close to the plasma membrane, and is believed to influence the deposition of cellulose microfibrils in the cell wall. The inelastic nature of cellulose restricts turgor-driven growth to the direction perpendicular to net microfibril orientation. In an elongating organ, such as a primary root, cells expand almost exclusively in length. Microtubules in these cells are arranged in parallel arrays perpendicular to the axis of elongation, typically reorienting to oblique as elongation ceases. Although there is uncertainty over the mechanism(s) whereby microtubules influence morphogenesis (Baskin 2001, Wasteneys 2004), it is indisputable that the cortical array of microtubules plays a profound role in creating the distinct shapes of higher plant organs.

Little is known about how plants organize microtubules, particularly on the organ-wide scale. Models have been proposed (e.g. Wasteneys 2002, Dixit and Cyr 2004), but these usually focus on local microtubule behavior and none can explain how microtubules in a field of cells can be oriented on average in a given direction. Several mutants have been identified that have defective microtubule organization; however, most of them affect the ability of cells to build organized arrays. For example, in *microtubule organization 1* (*mor1*), the cortical array consists of fewer, shorter and apparently less well organized microtubules than in wild-type plants (Whittington et al. 2001). Other mutants have extremely disorganized cortical microtubules, as in the case of *botero/fragile fiber 2* (*bot/fra2*: Bichet et al. 2001, Burk et al. 2001), *root epidermal bulger* (*reb/rhd1*: Andème-Onzighi et al. 2002) and *tonneau* (*ton*)/*fass*, which also lacks pre-prophase bands (Traas et al. 1995, Thion et al. 1998).

Interestingly, a few mutants are known in which microtubule organization is disrupted on a larger scale while maintaining organized microtubules on a cellular level. For example, the *spiral* and *lefty* mutants have obliquely oriented microtubules over a larger portion of the root's elongation zone compared with wild type, which evidently causes the root to twist (Furutani et al. 2000, Thitamadee et al. 2002). When the microtubule helix is oriented to the right, as in *lefty*, the root twists to the left, and vice versa in the *spiral* mutants.

* Corresponding author: E-mail, alexb@bio.umass.edu; Fax, +1-413-545-3243.

Here, we describe the mutant *radially swollen 6* (*rsw6*), focusing on cells in the root epidermis. In this tissue, microtubules in *rsw6* are organized into parallel arrays within cells, but neighboring cells frequently contain cortical arrays differing in their mean orientation by up to 90°. In addition, microtubules in *rsw6* compared with the wild type appear to be moderately more stable in the presence of the microtubule inhibitor, oryzalin.

Results

Genetics and mapping

To identify genes active in morphogenesis, Baskin et al. (1992) screened for temperature-dependent alteration in root morphology, and called mutants with this phenotype 'radially swollen' (*rsw*). Eight Rsw loci have been defined based on complementation analysis; among them, the mutant studied here, *rsw6*, isolated in the Columbia background, is recessive to Columbia wild type, monogenic and nuclear (Wiedemeier 1998). Three independent alleles were recovered with indistinguishable phenotypes. Analysis of F₂ progeny of a cross between *rsw6* and

Landsberg *erecta* reveals that the *RSW6* locus is closely linked to the simple sequence length polymorphism (SSLP) marker MBK-5 on the southern end of chromosome 5 (four recombinations among 342 chromosomes).

Morphology and growth rate of the rsw6 root

The screen for conditional Rsw phenotypes used 19°C as the permissive temperature and 30°C as the restrictive temperature. Although 30°C is near the upper end of tolerance for arabidopsis, few if any cytological anomalies have been reported at this temperature in wild-type roots, at least for exposures of several days or less (Lane et al. 2001, Williamson et al. 2001, Sugimoto et al. 2003). At 19°C, the morphology of *rsw6* roots generally resembled that of wild-type roots, except for a mild twisting of epidermal cell files (Fig. 1a, b) and, although epidermal cells were sometimes slightly rounded, root diameter was not significantly increased compared with wild type. In contrast, after transfer to 30°C, the root tips of *rsw6* seedlings became swollen, with individual epidermal cells bulging from the root surface, particularly in the elongation and mature zones (Fig. 1c). Within 6 h of transfer, cells on the surface of
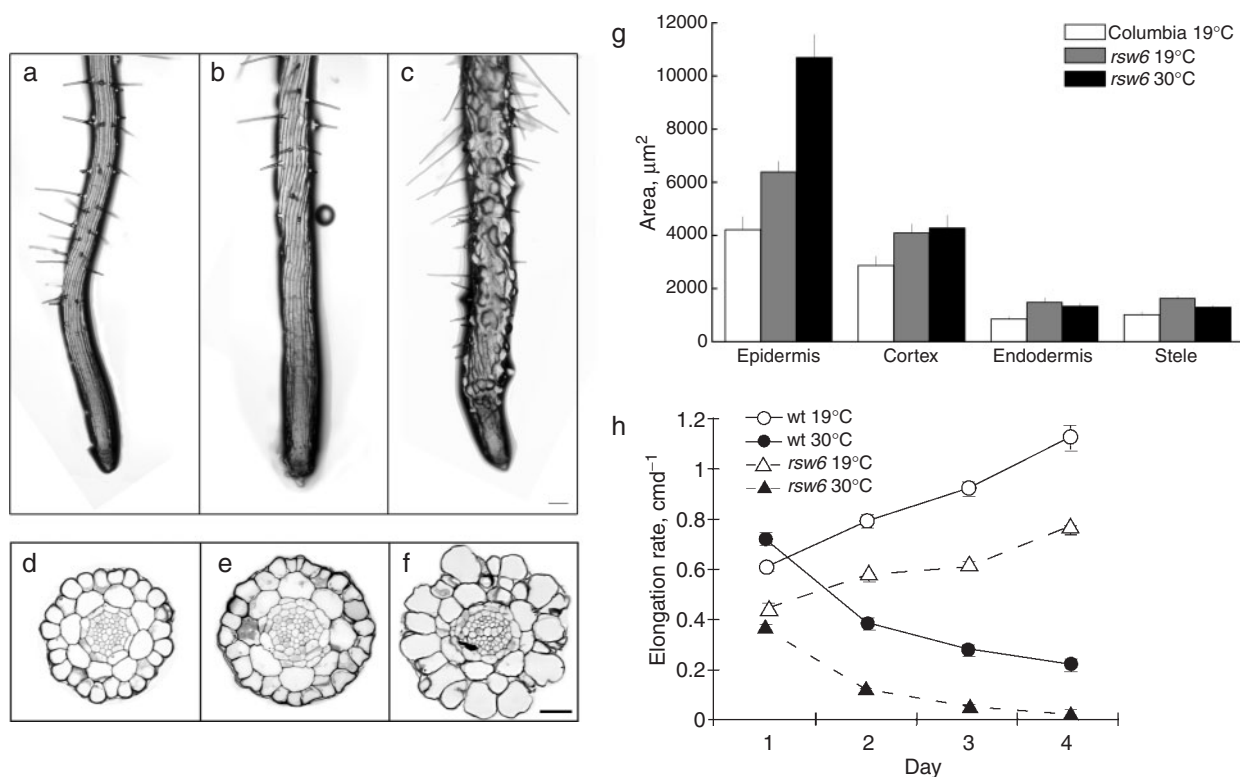

Fig. 1 Morphology, histology and growth of *rsw6* roots compared with wild type. (a) Wild type at 19°C. (b) *rsw6* at 19°C. (c) *rsw6* at 30°C for 1 d. (d–f) Methacrylate cross-sections stained to show cell walls. (d) Wild type at 19°C. (e) *rsw6* at 19°C. (f) *rsw6* at 30°C for 2 d. (g) Quantification of tissue areas from sections such as shown in (d–f). The cross-sectional areas of wild-type root tissues did not change at 30°C. Error bars show the SE. For the procedure used to quantify areas, see Materials and Methods. Scale bars: 100 μm (a–c), 32 μm (d–f). (h) Time course of the root elongation rate at 19°C or following transfer to 30°C at time zero. Symbols plot mean ± SE (when larger than the symbol) of three replicate experiments.

the root were noticeably swollen. After 48 h at 30°C, the cross-sectional areas of cortex, endodermis and stele in *rsw6* increased slightly, but the cross-sectional area of the epidermis increased by approximately 70% (Fig. 1d–g). Areas of the wild-type tissues are indistinguishable at the two temperatures (Williamson et al. 2001).

Roots of *rsw6* plants elongated more slowly than wild-type plants at both the permissive and restrictive temperatures (Fig. 1h). At 19°C, the elongation rate accelerated in both genotypes and *rsw6* maintained an elongation rate about 70% of the wild-type rate. In principle, this could reflect delayed germination in *rsw6*; however, germination assays ruled this out (data not shown). At 30°C, both wild-type and *rsw6* elongation rates decreased progressively with time, but *rsw6* was affected more severely. After 2 d at 30°C, *rsw6* roots elongated at about 50% the rate of the wild type, but by 4 d at 30°C, the mutant's elongation rate became barely measurable, while wild-type roots grew steadily, albeit slowly, at approximately $2\,\mathrm{mm\,d^{-1}}$.

Shoot phenotypes

The aerial parts of *rsw6* displayed mild phenotypes at 30°C, which included swelling of etiolated hypocotyls and less convoluted margins on leaf epidermal cells; however, trichomes, like root hairs, appeared normal. Microtubule orientation status in the hypocotyl was difficult to evaluate because, even in wild-type cells, the cortical array is not particularly well organized. Because the wild-type shoot is compromised at 30°C when plants are exposed for long enough to manifest shoot growth phenotypes, this report focuses on root phenotypes. Root phenotypes are pronounced even after a few hours, and the root is a convenient organ for characterizing microtubule behavior.

Microtubule orientation in the rsw6 root

At 19°C, cortical microtubules in root epidermal cells of *rsw6* closely resembled those of the wild type in density and organization (Fig. 2), with the exception that one or two cells could usually be found in the meristem in which microtubules, although parallel, were not transverse (Fig. 2b, arrowheads). Microtubules in wild-type roots transferred to 30°C for up to 6 h were apparently unaffected (Fig. 2c); in contrast, by 6 h after transfer to 30°C, microtubules in *rsw6* had notably aberrant alignment and, concomitantly, cells in the elongation zone were swollen (Fig. 2d). Although microtubule arrays were well organized in individual cells, the net orientation of the microtubules frequently differed between neighboring cells (Fig. 2d, arrowheads). In sectioned material, microtubule reorientation in *rsw6* was observed only in the epidermis (Wiedemeier 1998), consistent with the epidermis being the only swollen tissue.

These visual assessments were supported by quantifying the percentages of cells in the early elongation zone with arrays in various orientation classes. After 6 h of exposure to 30°C, <60% of cells in *rsw6* had transverse arrays (Fig. 2e, column iv). A time course showed that a significant degree of reorientation took place within 2 h of transfer to 30°C, reaching a maximum after about 4 h. After that, the degree of reorientation fluctuated across all time points
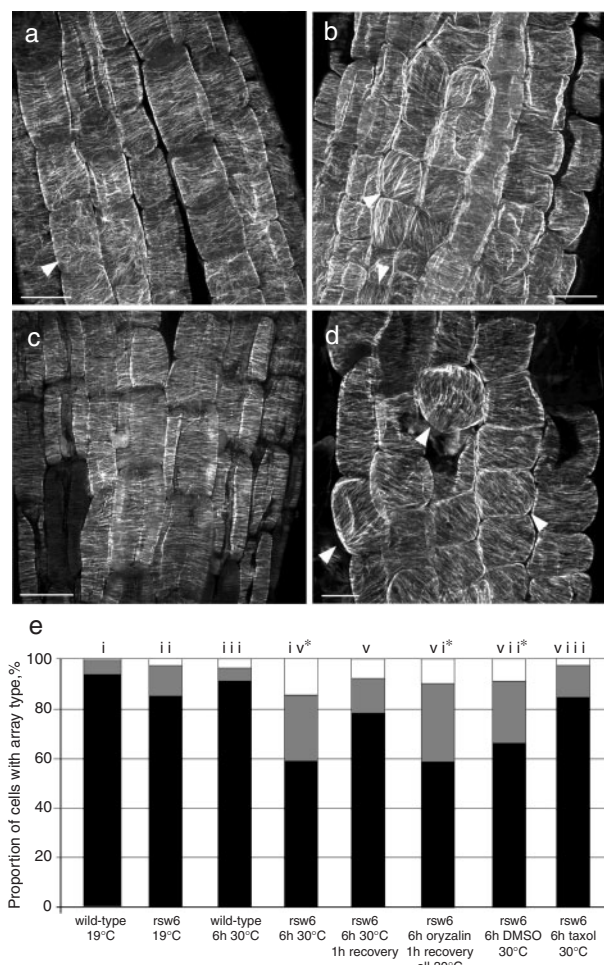

Fig. 2 Microtubule orientations in wild type and *rsw6*. (a–d) Confocal micrographs of immunolabeled microtubules in root epidermal cells. (a) Wild type at 19°C. The arrowhead shows an example of a cell with disorganized cortical microtubules, which were seen occasionally in this region. (b) *rsw6* at 19°C. Arrowheads show examples of cells with parallel but not transverse cortical microtubules. (c) Wild type after 6 h at 30°C. (d) *rsw6* incubated at 30°C for 6 h. A large proportion of cells have oblique and longitudinal microtubule arrays (arrowheads). Scale bars: 10 μm. (e) Microtubule array composition in wild type and *rsw6* at 19 and 30°C, and after treatment with 1 μM oryzalin or 20 μM taxol. Black, transverse; gray, oblique; white, longitudinal. Percentages are means of cells from 8–10 replicate roots. Asterisks denote a significant difference from *rsw6* at 19°C ($P<0.005$) by χ^2 test.

studied (up to 24 h), but the proportion of cells with transverse microtubules was always significantly lower than at 19°C (Bannigan 2003). In *rsw6* plants incubated at 30°C for 6 h and then returned to 19°C for 2 h, microtubules were restored to a predominantly transverse alignment, with the proportion of cells containing transverse arrays being not significantly different from plants grown at 19°C only (Fig. 2e, column v). The presence of microtubules per se is apparently not required for the development of the reoriented microtubule phenotype in *rsw6* roots, because when microtubules were depolymerized with 1 μM oryzalin for 6 h at 30°C, followed by drug removal for 1 h at 30°C, microtubule arrays resembled those in roots exposed to 30°C for 6 h (Fig. 2e, column vi; Fig. 6d).

To observe microtubule reorientation, we crossed *rsw6* into lines expressing green fluorescent protein (GFP)–β-tubulin (from David Ehrhardt, Carnegie Institution of Washington). Although this reporter gives rather intense background fluorescence in root cells, perhaps because of a high concentration of cytosolic tubulin, the signal is adequate to image microtubules. Confocal imaging of GFP–tubulin in *rsw6* roots after several hours at 30°C showed non-uniform microtubule organization, similar to that reported above for fixed cells (Fig. 3). Additionally, time-lapse observations revealed that the orientation of the array in many, but not all, cells continued to change while kept at 30°C.

Effect of taxol and oryzalin on growth and microtubule stability in *rsw6*

To assess the requirement for microtubule dynamics in the microtubule reorientation phenotype of the mutant, we transferred roots to 30°C in the presence of 20 μM taxol (Fig. 4). After 6 h, when *rsw6* roots exposed to dimethyl-sulfoxide (DMSO) alone had cells with reoriented microtubules, *rsw6* roots on taxol had mostly transverse microtubules. Quantification of microtubule orientations showed that array proportions in *rsw6* roots exposed to taxol for 6 h at 30°C were indistinguishable from those of *rsw6* at 19°C (Fig. 2e, column viii). In the wild type, taxol treatment did not quantitatively alter microtubule array orientations at either 19 or 30°C (not shown). Although conflicting reports have been published on the effect of taxol on microtubule reorientation (Weerdenburg and Seagull 1988, Baskin et al. 1994, Wymer et al. 1996), microtubule dynamics appear to be essential for reorientation in *rsw6*. Because taxol causes wild-type roots to swell (Baskin et al. 1994), we could not determine whether blocking reorientation with taxol would also block the swelling phenotype in *rsw6*.

To determine whether the mutation affects microtubule stability, we investigated the sensitivity of microtubules to depolymerization by oryzalin. In preliminary experiments
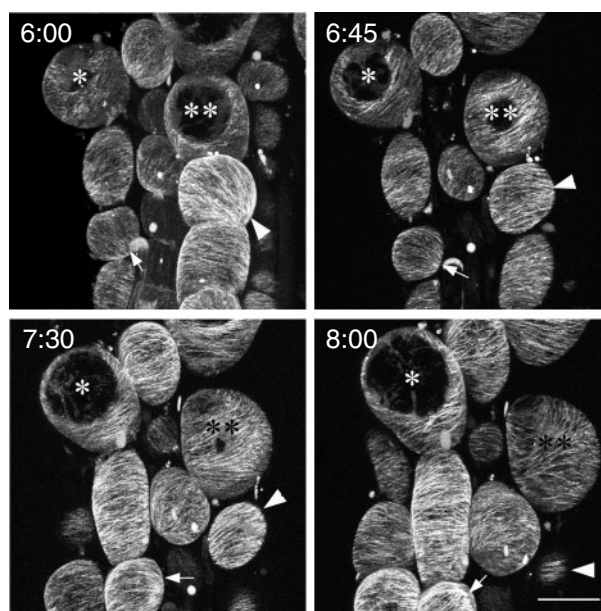

Fig. 3 Confocal micrographs of GFP–tubulin in an *rsw6* root, taken over the course of 2 h, starting at 6 h after exposure to 30°C. ∗ and ∗∗ indicate the same cells in all images. Arrows and arrowheads point to cells where orientation changed markedly in this period. The ongoing swelling and irregular growth of cells in this region precluded comprehensive tracking of orientations in all cells. Time in hours and minutes from transfer to 30°C is shown in the upper left corner. Scale bar: 20 μm.
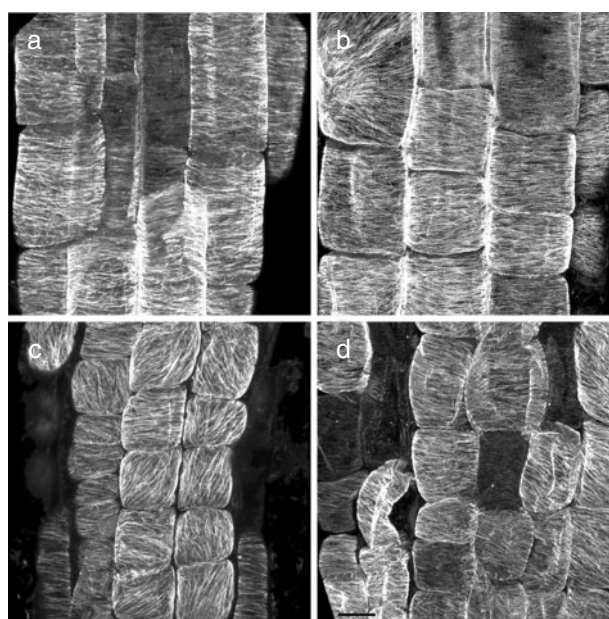

Fig. 4 Confocal micrographs of immunolabeled microtubules showing the effect of taxol on microtubule reorientation in *rsw6*. (a) Wild-type control (DMSO), 6 h at 30°C. (b) Wild type treated with 20 μM taxol for 6 h at 30°C. (c) *rsw6* control (DMSO), 6 h at 30°C. (d) *rsw6* treated with 20 μM taxol for 6 h at 30°C. Scale bar: 10 μm.

with GFP–tubulin plants, we found that 600 nM oryzalin affected microtubules rapidly enough for convenient observation but not so rapidly as to obscure differences between the genotypes. Wild-type roots at 19 and 30°C fixed after 20 min on 600 nM oryzalin had only very sparse microtubules in the epidermal cells (Fig. 5a–d). Cells in the treated roots had high background fluorescence, presumably from the antibody labeling tubulin oligomers in the cytoplasm. In contrast, *rsw6* roots fixed after 20 min on oryzalin, particularly those at 30°C, had considerably more microtubules remaining, along with little increase in background fluorescence (Fig. 5e–h). These observations were confirmed in living cells with the GFP–tubulin lines (not shown).

Additionally, microtubule recovery from oryzalin was studied in wild type and *rsw6* at 30°C. Microtubules were completely depolymerized by treatment with 1 µM oryzalin for 6 h, then roots were washed with Hoagland's solution for 1 h. By that time, cortical arrays in the wild type had recovered only partially (Fig. 6a, b) whereas those in the mutant appeared to have recovered fully (Fig. 6c, d).

To determine whether the oryzalin resistance observed in the short term correlated with a longer term effect on growth, we assayed the root elongation rate in the presence and absence of 600 nM oryzalin (Fig. 7a). Because the root elongation rate in *rsw6* differs from that of the wild type even at the permissive temperature, the data in Fig. 7a for each treatment are expressed as a percentage of the untreated elongation rate for the same day. While the genotypes responded in the same way to oryzalin at 19°C, *rsw6* was substantially resistant to oryzalin over the first 2 d of treatment at 30°C. With longer treatment, oryzalin brought the elongation rate of both genotypes close to zero, presumably because cell division ceased. In view of the resistance of *rsw6* to oryzalin, we tested *rsw6* for hypersensitivity to taxol; however, 20 µM taxol inhibited root elongation in *rsw6* and wild type indistinguishably (Fig. 7b). Because 20 µM taxol inhibits root elongation to approximately the same extent as does 600 nM oryzalin, the observed resistance of *rsw6* to oryzalin is unlikely to be simply a consequence of limitations in measuring the low growth rate of the mutant at the restrictive temperature.

Fig. 5 Confocal fluorescence micrographs comparing the effects of oryzalin on wild-type and *rsw6* roots. The left panel shows untreated roots; the right panel shows roots treated with 600 nM oryzalin for 20 min. (a, b) Wild-type at 19°C. (c, d) Wild type at 30°C. (e, f) *rsw6* at 19°C. (g, h) *rsw6* at 30°C. Scale bar: 20 µm.

Role of actin in the rsw6 microtubule reorientation phenotype

To assess actin organization in *rsw6*, we examined actin arrays with chemical fixation followed by immunostaining. Although the inherently irregular organization of actin in root cells makes it difficult to observe subtle changes, actin arrays in *rsw6* at 30°C generally resembled those at 19°C as well as those in the wild type (Bannigan 2003). Surprisingly, treatme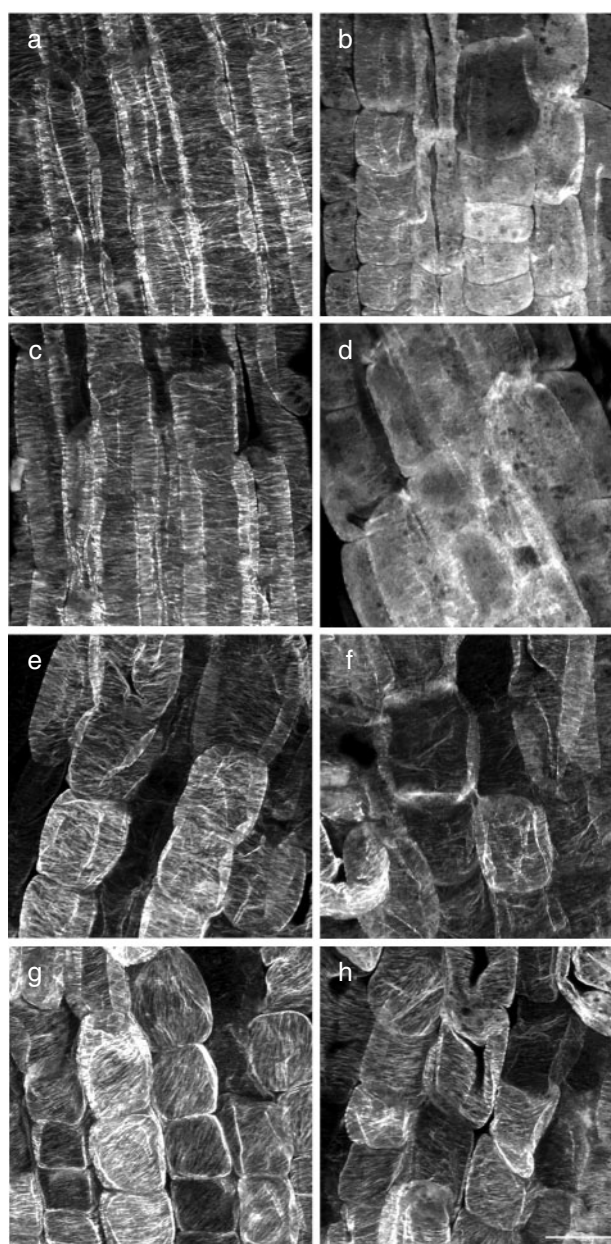nt of *rsw6* with 25 µM latrunculin B, which removed essentially all actin detectable by our protocol, minimized microtubule reorientation (Fig. 8c), indicating that an intact actin cytoskeleton is required for the development of misaligned microtubules in *rsw6*. Latrunculin also prevented reorientation of repolymerizing microtubules when applied simultaneously with oryzalin (Fig. 8d). However, latrunculin applied only during the recovery of oryzalin-treated microtubules did not prevent
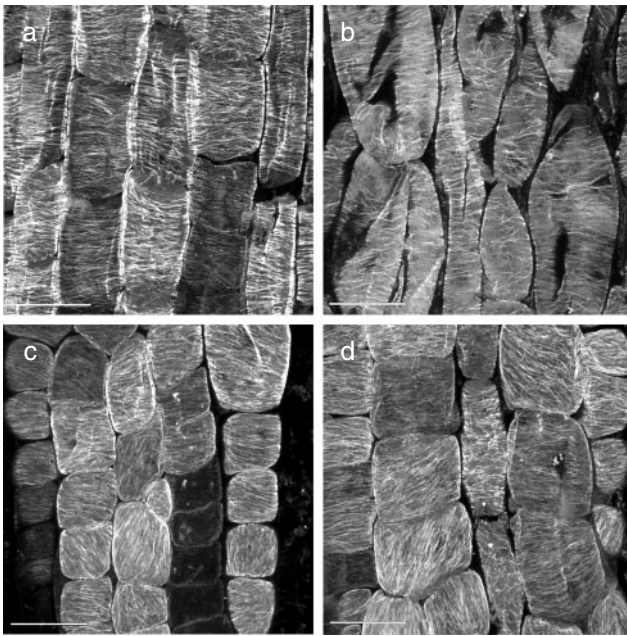
Fig. 6 Microtubule recovery from depolymerization in wild type and *rsw6*, all at 30°C. (a) Wild type and (c) *rsw6* treated with DMSO for 6 h, followed by 1 h recovery; (b) wild type and (d) *rsw6* treated with 1 μM oryzalin for 6 h, followed by 1 h recovery. Oryzalin (1 μM) caused complete depolymerization of microtubules in all of a subset of roots fixed before recovery. Scale bars: 20 μm.

Fig. 7 Time course of root elongation following exposure to 600 nM oryzalin (a) or 20 μM taxol (b) at time zero. Symbols plot the mean ± SE of three replicate plates from a single experiment. Elongation rates are expressed as a percentage of the rate for untreated seedlings, measured in the same experiment.

reorientation (Fig. 8e), suggesting that actin is important in the early stages of reorientation but not for directly positioning microtubules.

Discussion

The temperature-sensitive mutant, *rsw6*, was isolated in a screen for mutants exhibiting swollen root tips at 30°C. It is not allelic to the other known *rsw* mutants (Wiedemeier 1998). Growth of *rsw6* roots is slower than that of wild-type roots, even at the permissive temperature, indicating that 19°C is not fully permissive. At the restrictive temperature, root elongation is severely impaired, epidermal cells of the root swell and become rounded, and cortical microtubules in these cells become organized in parallel arrays of various orientations. Within individual cells, the microtubules remain parallel, perhaps even more so than in wild-type cells. Microtubules regain a global, transverse orientation upon return to the permissive temperature. Observation of *rsw6* roots expressing GFP–tubulin shows that the microtubule arrays in many cells continue to change orientation as long as the plant is kept at the restrictive temperature.

Intriguingly, the appearance of the microtubule arrays in the *rsw6* epidermis at 30°C resembles the usual state for the epidermis of stems, including the fluctuating
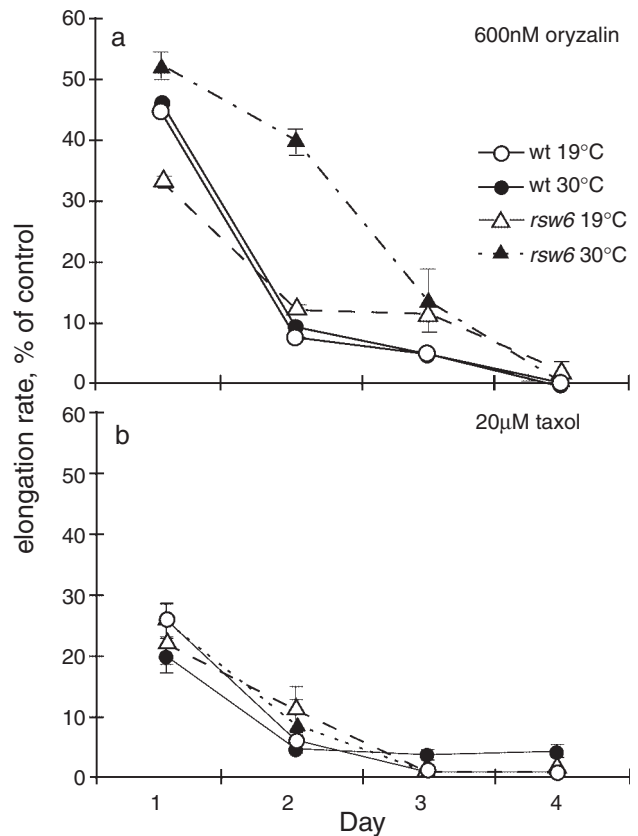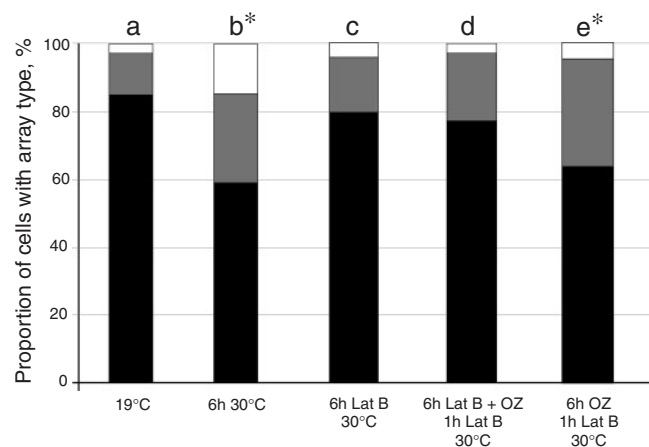

Fig. 8 Microtubule array composition in *rsw6* at 19 and 30°C, and after treatment with 1 μM oryzalin (OZ) and/or 25 μM latrunculin (latB) at 30°C, as indicated. Black, transverse; gray, oblique; white, longitudinal. Bars plot means of cells from 10–18 replicate roots. Asterisks denote significant difference from *rsw6* at 19°C ($P < 0.005$) by χ^2 test.

orientations (e.g. Takeda and Shibaoka 1981, Takesue and Shibaoka 1998). The fact that a patchwork alignment leads to epidermal swelling in the *rsw6* root but not in the wild-type stem could indicate an additional loss of function for microtubules in *rsw6* beyond aberrant orientation. Alternatively, the difference in swelling could indicate a difference in the role of the epidermis between stem and root. The outer epidermal wall in a growing stem is far thicker than the surrounding cell walls and has been interpreted as needing force supplied by the inner tissue to expand (Green 1980, Peters and Tomos 2000). The swelling of the root epidermis in *rsw6*, without appreciable concomitant swelling in interior tissues, demonstrates that the radial expansion of the root is neither limited by the epidermis nor driven by the expansion of interior tissues.

Microtubule organization, stability and relationship to actin

The *rsw6* mutant is unusual among microtubule mutants. Most microtubule mutants show either general disarray, as in *mor1* (Whittington et al. 2001) and *fra2/bot1* (Bichet et al. 2001, Burk et al. 2001), or misalignment of organized microtubules over an entire tissue, as in *spiral* (Furutani et al. 2000) and *lefty* (Thitamadee et al. 2002). Instead, *rsw6* has microtubules that are ordered within cells, but misaligned with respect to both the axis of the organ and surrounding cells in the same tissue. Another unusual trait of *rsw6* is that its microtubules are more resistant to depolymerization by oryzalin than those of the wild type. Both elongation rate and microtubule stability in *rsw6* roots are less affected by oryzalin than in the wild type, particularly at the restrictive temperature. Furthermore, repolymerization of microtubules after complete depolymerization with oryzalin is faster in *rsw6* than in the wild type. In contrast, other microtubule mutants (e.g. *lefty1*, *lefty2*, *spiral2*, *propyzamide hypersensitive1*) are all more sensitive to anti-microtubule drugs (Thitamadee et al. 2002, Naoi and Hashimoto 2004, Shoji et al. 2004), although dinitroaniline resistance has been reported in some crop species (Anthony and Hussey 1999). Preliminary experiments showed that both growth and microtubules in *rsw6* are partially resistant to the benzamide anti-microtubule drug, RH-4032 (Young and Lewandowski 2000), and scarcely resistant to colchicine. This spectrum of resistance may implicate a site on the microtubule lattice in conferring stability, but further experiments are required to pursue this point.

Interestingly, the only other mutant known to us to have apparently hyperstable microtubules is *distorted2*, although it is endoplasmic rather than cortical arrays that were shown to be stabilized (Saedler et al. 2004). This mutant lacks a functional ARP2/3 complex, which is fundamental for actin organization (Smith and Oppenheimer 2005), and therefore suggests that actin function and microtubule stability are linked (Saedler et al. 2004, Bannigan and Baskin 2005).

Several authors have suggested that actin plays a role in microtubule organization, for example in guiding the expanding phragmoplast (Lloyd 1999) or in directing the colonization of the cortex by microtubules following mitosis (Yoneda et al. 2004). The phenotype of *rsw6* underscores a link between actin and microtubule orientation. When actin in *rsw6* is depolymerized throughout incubation at the restrictive temperature, microtubules remain transverse. This suggests that reorientation is an active process, not simply a loss of orienting information. Furthermore, following oryzalin treatment, the reorientation of microtubules depends on the presence of actin during the initial incubation period (when microtubules are absent) but is independent of actin during recovery (when microtubules repolymerize). It seems that actin is important for reorientation only during the early stages of the process.

The global regulation of cytoskeletal order

A major question that the *rsw6* phenotype raises is how microtubule organization is normally coordinated between neighboring cells, and across tissues. This problem is more complex than recognizing an organ's axis or an external cue. In several reports, microtubules form intricate patterns that transcend cell boundaries (Hardham et al. 1980, Sakaguchi et al. 1988, Marc and Hackett 1989, Hush et al. 1990, Cleary and Smith 1998, Overall et al. 2001). Models of microtubule organization typically focus on self-organization through inter-microtubule interaction and the action of microtubule-associated proteins (Wasteneys 2002, Dixit and Cyr 2004). Although such mechanisms can explain how a microtubule array is constructed, they do not explain how these arrays are organized on a multicellular level. For trichomes and leaf pavement cells, pathways are being elucidated whereby cytoskeletal regulation is coordinated throughout a cell (Saedler et al. 2004, Fu et al. 2005). If intercellular components, such as BRICK1, a protein that affects actin organization non-cell autonomously (Frank et al. 2003), are added to such models they offer a paradigm for how cytoskeletal function could be coordinated over a larger scale, possibly reaching that of the organ.

Clearly, we are just beginning to understand the coordination of cell behavior across a tissue. Mechanisms by which three-dimensional information could be shared between cells are difficult to investigate. In the case of *rsw6*, we propose that microtubule organization is functional on a cellular level, but defective on a global scale. This mutant provides a unique system in which to study the complexities of cytoskeletal organization and its coordination in multicellular plants.

Materials and Methods

Plant material, growth rate assays and inhibitor treatments

Seeds of *Arabidopsis thaliana* L. (Heynh) were surface sterilized, rinsed and planted on agar plates containing 1% Bacto-agar (Difco) and 1–3% sucrose in Hoagland's solution (2 mM KNO$_3$, 5 mM Ca[NO$_3$]$_2$, 2 mM MgSO$_4$, 2 mM KH$_2$PO$_4$, 0.09 mM Fe-EDTA), sealed with micropore tape and placed vertically in a growth cabinet in constant light (approximately 100 μmol m^{-2} s^{-1}) at 19°C. Plants were used 6 d after plating unless otherwise stated.

The *rsw6* line was selected visually in the M$_2$ generation from the Columbia population mutagenized with ethylmethane sulfonate (EMS) described previously (Baskin et al. 1992). It was assigned to a novel locus on the basis of complemented F$_1$ progeny in pairwise crosses between other Rsw mutants (*rsw1*–*rsw8*) (Wiedemeier 1998). Material used for these studies has been backcrossed at least twice to wild type. Throughout this report, 'wild type' refers to the Columbia background. The GFP–tubulin reporter lines express GFP fused to the *A. thaliana* β-tubulin-6 gene and were made by David Ehrhardt (Carnegie Institution of Washington, Stanford, CA, USA), following the same strategy as previously described for the *A. thaliana* α-tubulin-5 gene (Shaw et al. 2003). Two transgenic lines expressing the GFP–tubulin reporter in the Columbia background, representing independent transformants with the same construct, were crossed onto *rsw6*. Lines homozygous for *rsw6* and brightly fluorescent were selected by visual inspection from the F$_2$ and bulked up.

Root elongation rates were measured on successive days by ticking the back of the Petri dish at the position of the root tip, as described by Baskin and Wilson (1997). Seedlings treated with inhibitors were transferred to fresh plates containing the relevant inhibitor, which were made by adding small volumes of a concentrated stock solution in DMSO to the molten agar. Controls received the same amount of DMSO (never more than 0.1%). Plates with inhibitors were made in the same way for assays of elongation rate as well as of the cytoskeleton. For recovery studies, seedlings were washed four times for 15 min in Hoagland's solution at the same temperature.

Measurement of tissue areas

Roots were fixed, embedded in methacrylate, serially sectioned, and stained to show cell walls, as described previously (Wiedemeier et al. 2002). Measurements of diameter were used to define the region where root swelling was maximal (or the base of the meristem for wild type and *rsw6* at 19°C). A line was drawn around the outer perimeter of the epidermis and of each interior tissue, following cellular boundaries. Areas were calculated from each perimeter, assuming circular geometry, as $P^2(4\pi)^{-1}$, where P is the length of the perimeter line, and tissue area was found by subtracting the area given by the outer perimeter from that given by the inner. Four to five roots were sectioned per treatment and five to six sections per root were measured. Means are shown $\pm$ SE.

Immunofluorescence localization of microtubules

Seedlings were fixed in 4% paraformaldehyde, 1% glutaraldehyde, 50 mM KPIPES and 1 mM CaCl$_2$ (pH 7) for 1 h and rinsed three times for 10 min each in PME (50 mM KPIPES, 5 mM EGTA, 2 mM MgSO$_4$). They were then digested with 0.1% pectinase and 0.01% pectolyase, in phosphate-buffered saline (PBS: 3 mM KH$_2$PO$_4$, 7 mM K$_2$HPO$_4$, 150 nM NaCl) for 15 min and rinsed three times for 5 min each in 10% glycerol and 0.2% Triton X-100 in PME. The cells were extracted with methanol at −20°C for 15 min, rehydrated by rinsing three times for 5 min in PBS, and incubated with 1/1,000 monoclonal anti-α-tubulin antibody raised in mouse (Sigma, St Louis, MO, USA) at 37°C overnight. After rinsing three times for 5 min in PBS, the roots were incubated with either 1/30 fluorescein isothiocyanate (FITC)-conjugated sheep anti-mouse antibody (Sigma) or 1/200 CY3-conjugated goat anti-mouse antibody (Jackson ImmunoResearch, West Chester, PA, USA) at 37°C for 3 h, rinsed again in PBS twice for 5 min each, mounted in Citifluor AF2 antifade (Alltech, Sydney, Australia) or Vectashield fluorescence mounting medium (Vector Laboratories; Burlingame, CA, USA), covered and sealed.

Immunofluorescence microscopy of whole roots was carried out using a Zeiss Axiovert inverted fluorescence microscope and a BioRad Radiance Plus or Zeiss 510C Meta Confocal microscope.

Microtubule orientation in fixed samples was quantified by visually categorizing cells in the apical part of the elongation zone, on the basis of their principal microtubule orientation, as transverse, oblique or longitudinal. The percentage of each array type was then calculated out of the total number of cells with clearly identifiable arrays. Between 300 and 500 cells from at least 10 different plants from each treatment were analyzed for microtubule organization. The significance of the degree of microtubule reorientation was assessed by comparing the proportion of cells retaining transverse arrays in different treatments using the χ^2 test, with differences with $P < 0.005$ considered significant.

Imaging GFP–tubulin

Seedlings expressing GFP–tubulin were gently transferred to welled Petri dishes, held in place with a small square of 2% Hoagland's agar, and moistened with a small drop of Hoagland's solution. In experiments with oryzalin, the mounting agar and Hoagland's solution both contained 600 nM oryzalin. When imaging live plants after 4–6 h at 30°C, a heated stage and objective were used to maintain the temperature throughout the experiment. Microtubule reorientation was imaged by capturing time series images on a Zeiss 510C Meta confocal microscope.

References

Andème-Onzighi, C., Sivaguru, M., Judy-March, J., Baskin, T.I. and Driouich, A. (2002) The reb1-1 mutation of Arabidopsis alters the morphology of trichoblasts, the expression of

arabinogalactan-proteins and the organization of cortical microtubules. *Planta* 215: 949–958.

Anthony, R.G. and Hussey, P.J. (1999) Dinitroaniline herbicide resistance and the microtubule cytoskeleton. *Trends Plant Sci.* 4: 112–116.

Bannigan, A. (2003) The relationship between intercellular communication and microtubule organization in plants. PhD thesis. University of Sydney, Australia.

Bannigan, A. and Baskin, T.I. (2005) Directional cell expansion—turning towards actin. *Curr. Opin. Plant Biol.* 8: 619–624.

Baskin, T.I. (2001) On the alignment of cellulose microfibrils by cortical microtubules: a review and a model. *Protoplasma* 215: 150–171.

Baskin, T.I., Batzner, A.S., Hoggart, R., Cork, A. and Williamson, R.E. (1992) Root morphology mutants in *Arabidopsis thaliana*. *Aust. J. Plant Physiol.* 19: 427–437.

Baskin, T.I. and Wilson, J.E. (1997) Inhibitors of protein kinases and phosphatases alter root morphology and disorganize cortical microtubules. *Plant Physiol.* 113: 493–502.

Baskin, T.I., Wilson, J.E., Cork, A. and Williamson, R.E. (1994) Morphology and microtubule organization in Arabidopsis roots exposed to oryzalin or taxol. *Plant Cell Physiol.* 35: 935–942.

Bichet, A., Desnos, T., Turner, S., Grandjean, O. and Höfte, H. (2001) *BOTERO1* is required for normal orientation of cortical microtubules and anisotropic cell expansion in *Arabidopsis*. *Plant J.* 25: 137–148.

Burk, D.H., Liu, B., Zhong, R., Morrison, W.H. and Ye, Z.H. (2001) A katanin-like protein regulates normal cell wall biosynthesis and cell elongation. *Plant Cell* 13: 807–827.

Cleary, A.L. and Smith, L.G. (1998) The *tangled1* gene is required for spatial control of cytoskeletal arrays associated with cell division during maize leaf development. *Plant Cell* 10: 1875–1888.

Dixit, R. and Cyr, R. (2004) The cortical microtubule array: from dynamics to organization. *Plant Cell* 16: 2546–2552.

Frank, M.J., Cartwright, H.N. and Smith, L.G. (2003) Three Brick genes have distinct functions in a common pathway promoting polarized cell division and cell morphogenesis in maize leaf development. *Development* 130: 753–762.

Fu, Y., Gu, Y., Zheng, Z., Wasteneys, G. and Yang, Z. (2005) *Arabidopsis* interdigitating cell growth requires two antagonistic pathways with opposing action on cell morphogenesis. *Cell* 120: 687–700.

Furutani, I., Watanabe, Y., Prieto, R., Masukawa, M., Suzuki, K., Naoi, K., Thitamadee, S., Shikanai, T. and Hashimoto, T. (2000) The SPIRAL genes are required for directional control of cell elongation in *Arabidopsis thaliana*. *Development* 127: 4443–4453.

Green, P.B. (1980) Organogenesis—a biophysical view. *Annu. Rev. Plant Physiol.* 31: 51–82.

Hardham, A.R., Green, P.B. and Lang, J.M. (1980) Reorganization of cortical microtubules and cellulose deposition during leaf formation in *Graptopetalum paraguayense*. *Planta* 149: 181–195.

Hush, J.M., Hawes, C.R. and Overall, R.L. (1990) Interphase microtubule re-orientation predicts a new cell polarity in wounded pea roots. *J. Cell Sci.* 96: 47–61.

Lane, D.R., Wiedemeier, A., Peng, L., Höfte, H., Hocart, C.H., Birch, R.J., Baskin, T.I., Burn, J.E., Arioli, T., Betzner, A.S. and Williamson, R.E. (2001) Temperature-sensitive alleles of radially swollen2 link the KORRIGAN endo-1,4-β-glucanse to cellulose synthesis and cytokinesis. *Plant Physiol.* 126: 278–288.

Lloyd, C. (1999) How I learned to love carrots: the role of the cytoskeleton in shaping plant cells. *BioEssays* 21: 1061.

Marc, J. and Hackett, W.P. (1989) A new method for immuno-fluorescent localization of microtubules in surface cell layers: application to the shoot apical meristem of *Hedera*. *Protoplasma* 148: 70–79.

Naoi, K. and Hashimoto, T. (2004) A semidominant mutation in an Arabidopsis mitogen-activated protein kinase phosphatase-like gene compromises cortical microtubule organization. *Plant Cell* 16: 1841–1853.

Overall, R.L., Dibbayawan, T.P. and Blackman, L.M. (2001) Intercellular alignments of the plant cytoskeleton. *J. Plant Growth Regul.* 20: 162–169.

Peters, W.S. and Tomos, A.D. (2000) The mechanic state of 'inner tissue' in the growing zone of sunflower hypocotyls and the regulation of its growth rate following excision. *Plant Physiol.* 123: 605–612.

Saedler, R., Mathur, N., Srinivas, B.P., Kernebeck, B., Hulskamp, M. and Mathur, J. (2004) Actin control over microtubules suggested by *DISTORTED2* encoding the *Arabidopsis* ARPC2 subunit homolog. *Plant Cell Physiol.* 45: 813–822.

Sakaguchi, S., Hogetsu, T. and Hara, N. (1988) Arrangement of cortical microtubules in the shoot apex of *Vinca major* L. *Planta* 175: 403–411.

Shaw, S.L., Kamyar, R. and Ehrhardt, D.W. (2003) Sustained microtubule treadmilling in Arabidopsis cortical arrays. *Science* 300: 1715–1718.

Shoji, T., Narita, N.N., Hayashi, K., Asada, J., Hamada, T., Sonobe, S., Nakajima, K. and Hashimoto, T. (2004) Plant-specific microtubule-associated protein SPIRAL2 is required for anisotropic growth in Arabidopsis. *Plant Physiol.* 136: 3933–3944.

Smith, L.G. and Oppenheimer, D.G. (2005) Spatial control of cell expansion by the plant cytoskeleton. *Annu. Rev. Cell Dev. Biol.* 21: 271–295.

Sugimoto, K., Himmelspach, R., Williamson, R.E. and Wasteneys, G.O. (2003) Mutation or drug-dependent micro-tubule disruption causes radial swelling without altering parallel cellulose microfibril deposition in arabidopsis root cells. *Plant Cell* 15: 1414–1429.

Takeda, K. and Shibaoka, H. (1981) Changes in microfibril arrangement on the inner surface of the epidermal cell walls in the epicotyl of *Vigna angularis* Ohwi et Ohashi during cell growth. *Planta* 151: 385–392.

Takesue, K. and Shibaoka, H. (1998) The cyclic reorientation of cortical microtubules in epidermal cells of azuki bean epicotyls: the role of actin filaments in the progression of the cycle. *Planta* 205: 539–546.

Thion, L., Mazars, C., Nacry, P., Bouchez, D., Moreau, M., Ranjeva, R. and Thuleau, P. (1998) Plasma membrane depolarization-activated calcium channels, stimulated by micro-tubule-depolymerizing drugs in wild-type *Arabidopsis thaliana* protoplasts, display constitutively large activities and a longer half-life in *ton* 2 mutant cells affected in the organization of cortical microtubules. *Plant J.* 13: 603–610.

Thitamadee, S., Tuchiara, K. and Hashimoto, T. (2002) Microtubule basis for left-handed helical growth in *Arabidopsis*. *Nature* 417: 193–196.

Traas, J., Bellini, C., Nacry, P., Kronenberger, J., Bouchez, D. and Caboche, M. (1995) Normal differentiation patterns in plants lacking microtubular preprophase bands. *Nature* 375: 676–677.

Wasteneys, G.E. (2002) Microtubule organization in the green kingdom: chaos or self order? *J. Cell Sci.* 115: 1345–1354.

Wasteneys, G.O. (2004) Progress in understanding the role of microtubules in plant cells. *Curr. Opin. Plant Biol.* 7: 651–660.

Weerdenburg, C. and Seagull, R.W. (1988) The effects of taxol and colchicine on microtubule and microfibril arrays in elongating plant cells in culture. *Can. J. Bot.* 66: 1707–1716.

Whittington, A.T., Vugrek, O., Wei, K.J., Hasenbein, N.G., Sugimoto, K., Rashbrooke, M.C. and Wasteneys, G.O. (2001) MOR1 is essential for organizing cortical microtubules in plants. *Nature* 411: 610–613.

Wiedemeier, A.M.D. (1998) Analysis of *Arabidopsis thaliana* growth anisotropy mutants: genetic, physiological and cytological characterization. PhD Thesis. University of Missouri, Columbia, USA.

Wiedemeier, A.M.D., Judy-March, J.E., Hocart, C.H., Wasteneys, G.O., Williamson, R.E. and Baskin, T.I. (2002) Mutant alleles of arabidopsis RADIALLY SWOLLEN 4 and RSW7 reduce growth anisotropy without altering the transverse orientation of cortical microtubules or cellulose microfibrils. *Development* 129: 4821–4830.

Williamson, R.E., Burn, J.E., Birch, R., Baskin, T.I., Arioli, T., Betzner, A.S. and Cork, A. (2001) Morphogenesis in *rsw1*, a cellulose-deficient mutant of *Arabidopsis thaliana*. *Protoplasma* 215: 116–127.

Wymer, C.L., Fisher, D.D., Moore, R.C. and Cyr, R.J. (1996) Elucidating the mechanism of cortical microtubule reorientation in plant cells. *Cell Motil. Cytoskel* 35: 162–173.

Yoneda, A., Akatsuka, M., Kumagai, F. and Hasezawa, S. (2004) Disruption of actin microfilaments causes cortical microtubule disorganization and extra phragmoplast formation at the M/G_1 interface in synchronized tobacco cells. *Plant Cell Physiol.* 45: 761–769.

Young, D.H. and Lewandowski, V.T. (2000) Covalent binding of the benzamide RH-4032 to tubulin in suspension-cultured tobacco cells and its application in a cell-based competitive-binding assay. *Plant Physiol.* 124: 115–124.